Earthquakes and Structures, *Vol. 10, No. 6 (2016) 1429-1449*
DOI: http://dx.doi.org/10.12989/eas.2016.10.6.1429

Effect of porosity on the bending and free vibration response of functionally graded plates resting on Winkler-Pasternak foundations

Rabia Benferhat*[1], Tahar Hassaine Daouadji[2], Mohamed Said Mansour[1] and Lazreg Hadji[2]

[1]*Laboratoire de Géomatériaux, Département de Génie Civil, Université Hassiba Benbouali de Chlef, Algérie*
[2]*Département de Génie Civil, Université Ibn Khaldoun de Tiaret, Algérie*

(Received January 5, 2016, Revised May 14, 2016, Accepted May 21, 2016)

Abstract. The effect of porosity on bending and free vibration behavior of simply supported functionally graded plate reposed on the Winkler-Pasternak foundation is investigated analytically in the present paper. The modified rule of mixture covering porosity phases is used to describe and approximate material properties of the FGM plates with porosity phases. The effect due to transverse shear is included by using a new refined shear deformation theory. The number of unknown functions involved in the present theory is only four as against five or more in case of other shear deformation theories. The Poisson ratio is held constant. Based on the sinusoidal shear deformation theory, the position of neutral surface is determined and the equation of motion for FG rectangular plates resting on elastic foundation based on neutral surface is obtained through the minimum total potential energy and Hamilton's principle. The convergence of the method is demonstrated and to validate the results, comparisons are made with the available solutions for both isotropic and functionally graded material (FGM). The effect of porosity volume fraction on Al/Al2O3 and Ti-6Al-4V/Aluminum oxide plates are presented in graphical forms. The roles played by the constituent volume fraction index, the foundation stiffness parameters and the geometry of the plate is also studied.

Keywords: porosity coefficient; FGM plate; bending and free vibration behavior; elastic foundation

1. Introduction

Materials, energy and modern science are three pillars of modern technology. New material development and researches are leading the invention of materials, as the cornerstone of the 21st century high-tech field. In recent years, materials science has gained rapid development (Pindera *et al.* 1994). Functionally graded materials (FGMs) are a new generation of engineered materials in which the microstructural details are spatially varied through non-uniform distribution of the reinforcement phase(s), by using reinforcement with different properties, sizes and shapes, as well as by interchanging the roles of reinforcement and matrix phases in a continuous manner (Hirai 1996).

*Corresponding author, Ph.D. Student, E-mail: rabiebenferhat@yahoo.fr

http://www.techno-press.com/journals/eas&subpage=7 ISSN: 2092-7614 (Print), 2092-7622 (Online)

The use of functionally graded materials in applications involving severe thermal gradients is quickly gaining acceptance in the composite mechanics community and the aerospace and aircraft industry. This is particularly true in Japan and Europe, where the concept of FGMs was conceived.

The components of structures widely used in aircraft, reusable space transportation vehicles and civil engineering are usually supported by an elastic foundation (Nguyen *et al*. 2013). Therefore, it is necessary to account for the effects of elastic foundation for a better understanding of the bending and free vibration behavior of plates and shells.

To describe the interaction between plate and foundation, various kinds of foundation models have been proposed, the Pasternak model (Pasternak 1954) or the two-parameter model is widely adopted to describe the mechanical behavior of foundations, and the well known Winkler model is one of its special cases. In fact, the two-parameter of elastic foundation models have been developed to overcome the inadequacy of Winkler model in describing the real soil response and the mathematical complexity of the three-dimensional continuum. The two-parameter model (Pasternak model) considers the shear deformation between the springs over the one-parameter model whilst the one-parameter model (Winkler model) can be represented by continuous springs. Therefore, Winkler model can be considered as a special case of Pasternak model by setting the shear modulus to zero.

However, in FGM fabrication, micro voids or porosities can occur within the materials during the process of sintering. This is because of the large difference in solidification temperatures between material constituents (Zhu *et al.* 2001). Wattanasakulpong *et al.* (2012) also gave the discussion on porosities happening inside FGM samples fabricated by a multi-step sequential infiltration technique. Therefore, it is important to take into account the porosity effect when designing FGM structures subjected to dynamic loadings (Wattanasakulpong *et al.* 2014).

Therefore, based on the above discussion, many researchers have paid more attention on investigating mechanical response of FGM plates and beams. Talha *et al.* (2010) studied the free vibration and static analysis of functionally graded material (FGM) plates using higher order shear deformation theory with a special modification in the transverse displacement in conjunction with finite element models. Gan *et al.* (2015) studied a finite element procedure for dynamic analysis of non-uniform Timoshenko beams made of axially Functionally Graded Material (FGM) under multiple moving point loads. Brischetto (2013) presented an exact three-dimensional elastic model for the free vibration analysis of functionally graded one-layered and sandwich simply-supported plates and shells. An exact closed-form solution is presented by Hosseini-Hashemi *et al.* (2011b) for moderately thick Lévy FGM plate. Efraim *et al.* (2007) presented the vibration analysis of thick annular plates with variable thickness made of isotropic material and FGM. Pradhan *et al.* (2015) studied the free vibration of functionally graded thin elliptic plates with various edge supports and the Rayleigh-Ritz technique is used to obtain the generalized eigenvalue problem. Kitipornchai *et al.* (2004) investigated the nonlinear vibration of imperfect shear deformable laminated rectangular plates comprising a homogeneous substrate and two layers of functionally graded materials (FGMs). Dozio (2014) derived first-known exact solutions for free vibration of thick and moderately thick functionally graded rectangular plates with at least one pair of opposite edges simply-supported on the basis of a family of two-dimensional shear and normal deformation theories with variable order. Carrera *et al.* (2010) investigated the static response problem of multilayered plates and shells embedding functionally graded material (FGM) layers. Carrera's unified formulation (CUF) is employed to obtain several hierarchical refined and advanced two-dimensional models for plates and shells. Bakora *et al.* (2015) investigated the postbuckling of thick plates made of functionally graded material (FGM) subjected to in-plane compressive,

thermal and thermomechanical loads. Brischetto *et al.* studied functionally graded material (FGM) plates subjected to a transverse mechanical load and the unified formulation (UF) and the Reissner's mixed variational theorem (RMVT) are extended to FGMs. Fazzolari *et al*. (2014) developed A fully coupled thermoelastic formulation to deal with free vibration analysis of anisotropic composite plates and isotropic/sandwich FGM plates. Thai *et al.* (2012) developed a refined shear deformation theory for free vibration of functionally graded plates on elastic foundation. Recently, by employing a novel four variables refined plate theory against five in case of other shear deformation theories, some studies (Belabed *et al.* 2014, Tounsi *et al.* 2013, Hamidi *et al.* 2015, Bennai *et al.* 2015, Bousahla *et al.* 2014) investigated the mechanical and theromechanical behavior of FG structures. Meksi *et al.* (2014) developed a novel simple first-order shear deformation plate theory based on neutral surface position for bending and free vibration analysis of functionally graded plates and supported by either Winkler or Pasternak elastic foundations. Hasani Baferani *et al.* (2011) use the third-order plate model to present Lévy-type solutions of rectangular FGM plates resting on elastic foundation. Thai *et al.* (2014) presented a zeroth-order shear deformation theory for bending and vibration analyses of functionally graded plates resting on elastic foundation. Ait Athmane *et al.* (2015) studied the effect of thickness stretching and porosity on mechanical response of a functionally graded beams resting on elastic foundations with the use of an efficient beam theory for bending, free vibration and buckling analysis.

The objective of this investigation is to present a new refined shear deformation theory for bending and free vibration response of simply supported functionally graded plate with porosities reposed on the elastic foundation. The effect due to porosity is included by using a modified rule of mixture covering porosity phases proposed by Wattanasakulpong *et al.* (2012). The material properties of FG plate are assumed to vary according to a power law distribution of the volume fraction of the constituents. The equation of motion for FGM plates is obtained through the minimum total potential energy and Hamilton's principle. The effects of varying power law index, volume fraction of porosity, aspect and side-to-thickness ratios on the bending and free vibration of FG plates are discussed. Some illustrative examples are also presented to verify the present formulation and solutions. Good agreement is observed.

2. Geometric configuration and material properties

Here we consider an FGM plate of length a, width b and total thickness h made of a mixture of metal and ceramics, in which the composition is varied from the top to the bottom surface. The material in top surface and in bottom surface is ceramic and metal respectively. To identify the location of neutral surface of FG plates, two different plans are taken into account for the measurement of z, namely z_{ms} and z_{ns} measured from the middle surface and the neutral surface of the plate, respectively as shown in Fig. 1.

In this study, we consider an imperfect FGM plate with a porosity volume fraction, α (α<<1), distributed uniformly among the metal and ceramic, the modified rule of mixture proposed by Wattanasakulpong and Ungbhakorn (2014) is used as

$$P = P_m\left(V_m - \frac{\alpha}{2}\right) + P_c\left(V_c - \frac{\alpha}{2}\right) \tag{1}$$

The power law of volume fraction of the ceramic is assumed as

$$V_c = (\frac{z_{ns}+c}{h}+\frac{1}{2})^k \tag{2}$$

The modified rule of mixture becomes

$$P=(P_c-P_m)(\frac{z_{ns}+c}{h}+\frac{1}{2})^k+P_m-(P_c+P_m)\frac{\alpha}{2} \tag{3}$$

It is noted that k is the power law index that takes values greater than or equals to zero. The FG plate becomes a fully ceramic plate when k is set to zero and fully metal for large value of k.

The Young's modulus (E) and density (ρ) of the imperfect FG can be written as a functions of thickness coordinate, z_{ns} , as follows (Ait Athmane *et al.* 2015a, b, Ait Yahia *et al.* 2015, Hadji *et al.* 2015a, b)

$$\begin{aligned} E(z) &= (E_c-E_m)(\frac{z_{ns}+c}{h}+\frac{1}{2})^k+E_m-(E_c+E_m)\frac{\alpha}{2} \\ \rho(z) &= (\rho_c-\rho_m)(\frac{z_{ns}+c}{h}+\frac{1}{2})^k+\rho_m-(\rho_c+\rho_m)\frac{\alpha}{2} \end{aligned} \tag{4}$$

The parameter C is the distance of neutral surface from the middle surface. However, the material properties of a perfect FG plate can be obtained when the volume fraction of porosity α is set to zero. Due to the small variations of the Poisson's ratio v, it is assumed to be constant

The position of the neutral surface of the FG plate is determined to satisfy the first moment with respect to Young's modulus being zero as follows (Zhang *et al.* 2008, Prakash *et al.* 2009, Bodaghi *et al.* 2011)

$$\int_{-h/2}^{h/2} E(z_{ms})(z_{ms}-C)dz_{ms}=0 \tag{5}$$

Consequently, the position of neutral surface can be obtained as (Bodaghi *et al.* 2011)

$$C=\frac{\int_{-h/2}^{h/2} E(z_{ms})z_{ms}\,dz_{ms}}{\int_{-h/2}^{h/2} E(z_{ms})\,dz_{ms}} \tag{6}$$

It can be seen that the physical neutral surface and the geometric middle surface are the same in a homogeneous isotropic plate.

3. Displacement field and strains

Based on the higher order shear deformation plate theory, the displacement components are

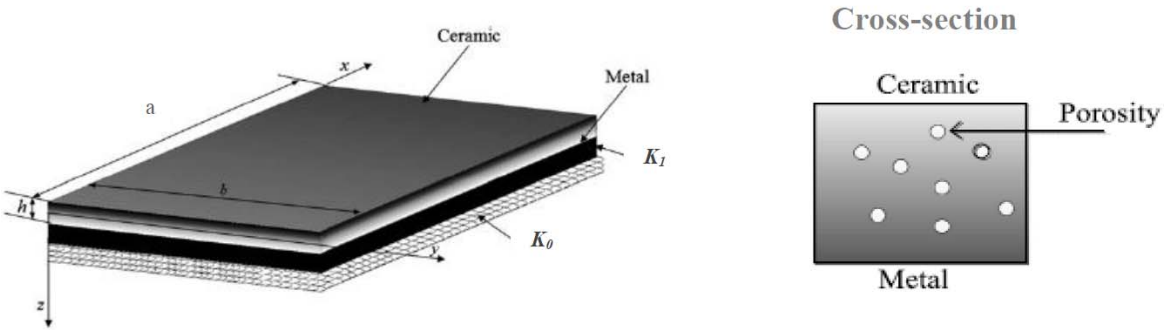

Fig. 1 Geometry and dimensions of the FGM plate resting on elastic foundation

assumed to be

$$\begin{aligned} u(x,y,z_{ns}) &= u_0(x,y) - z_{ns}\frac{\partial w_b}{\partial x} - f(z_{ns})\frac{\partial w_s}{\partial x} \\ v(x,y,z_{ns}) &= v_0(x,y) - z_{ns}\frac{\partial w_b}{\partial y} - f(z_{ns})\frac{\partial w_s}{\partial y} \\ w(x,y,z_{ns}) &= w_b(x,y) + w_s(x,y) \end{aligned} \tag{7}$$

The origin of the material coordinates is at the neutral surface of the plate. The linear strain can be obtained from kinematic relations as

$$\begin{aligned} \varepsilon_x &= \varepsilon_x^0 + z_{ns}\, k_x^b + f(z_{ns})\, k_x^s \\ \varepsilon_y &= \varepsilon_y^0 + z_{ns}\, k_y^b + f(z_{ns})\, k_y^s \\ \gamma_{xy} &= \gamma_{xy}^0 + z_{ns}\, k_{xy}^b + f(z_{ns})\, k_{xy}^s \\ \gamma_{yz} &= g(z_{ns})\, \gamma_{yz}^s \\ \gamma_{xz} &= g(z_{ns})\, \gamma_{xz}^s \\ \varepsilon_z &= 0 \end{aligned} \tag{8}$$

Where

$$\begin{gathered} \varepsilon_x^0 = \frac{\partial u_0}{\partial x}, \quad k_x^b = -\frac{\partial^2 w_b}{\partial x^2}, \quad k_x^s = -\frac{\partial^2 w_s}{\partial x^2} \\ \varepsilon_y^0 = \frac{\partial v_0}{\partial y}, \quad k_y^b = -\frac{\partial^2 w_b}{\partial y^2}, \quad k_y^s = -\frac{\partial^2 w_s}{\partial y^2} \\ \gamma_{xy}^0 = \frac{\partial u_0}{\partial y} + \frac{\partial v_0}{\partial x}, \quad k_{xy}^b = -2\frac{\partial^2 w_b}{\partial x \partial y}, \quad k_{xy}^s = -2\frac{\partial^2 w_s}{\partial x \partial y} \\ \gamma_{yz}^s = \frac{\partial w_s}{\partial y}, \quad \gamma_{xz}^s = \frac{\partial w_s}{\partial x}, \quad g(z_{ns}) = 1 - f'(z_{ns}), \quad f'(z_{ns}) = \frac{df(z_{ns})}{dz_{ns}} \\ f(z) = z_{ns} + C - \sin\left(\frac{\pi(z_{ns}+C)}{h}\right) \end{gathered} \tag{9}$$

The linear constitutive relations of a FG plate can be written as

$$\begin{Bmatrix} \sigma_x \\ \sigma_y \\ \tau_{xy} \end{Bmatrix} = \begin{bmatrix} Q_{11} & Q_{12} & 0 \\ Q_{12} & Q_{22} & 0 \\ 0 & 0 & Q_{66} \end{bmatrix} \begin{Bmatrix} \varepsilon_x \\ \varepsilon_y \\ \gamma_{xy} \end{Bmatrix}$$
$$\begin{Bmatrix} \tau_{yz} \\ \tau_{zx} \end{Bmatrix} = \begin{bmatrix} Q_{44} & 0 \\ 0 & Q_{55} \end{bmatrix} \begin{Bmatrix} \gamma_{yz} \\ \gamma_{zx} \end{Bmatrix} \tag{10}$$

Where

$$Q_{11} = Q_{22} = \frac{E(z_{ns})}{1-\nu^2}$$
$$Q_{12} = \frac{\nu E(z_{ns})}{1-\nu^2} \tag{11}$$
$$Q_{44} = Q_{55} = Q_{66} = \frac{E(z_{ns})}{2(1+\nu)}$$

4. Equations of motion

In order to obtain the equations of motion, the energy method is adopted and the total energy of structure is required

$$U = \frac{1}{2}\int_V \sigma_{ij}\varepsilon_{ij}\,dV = \frac{1}{2}\int_V (\sigma_x\varepsilon_x + \sigma_y\varepsilon_y + \sigma_{xy}\gamma_{xy} + \sigma_{yz}\gamma_{yz} + \sigma_{xz}\gamma_{xz})\,dV \tag{12a}$$

Also, using the Hamilton's principle, the governing equations of motion can be obtained as

$$0 = \delta\int_{t_1}^{t_2} (U + U_F - K - W)\,dt \tag{12b}$$

Where U is the strain energy and K is the kinetic energy of the FG plate, U_F is the strain energy of foundation and W is the work of external forces. Employing the minimum of the total energy principle leads to a general equation of motion and boundary conditions. Taking the variation of the above equation and integrating by parts

$$\int_{t_1}^{t_2}\left[\int_V [\sigma_x\delta\varepsilon_x + \sigma_y\delta\varepsilon_y + \tau_{xy}\delta\gamma_{xy} + \tau_{yz}\delta\gamma_{yz} + \tau_{zx}\delta\gamma_{zx} - \rho(\ddot{u}\delta u + \ddot{v}\delta v + \ddot{w}\delta w)dv + \int_A [f_e\delta w]dA\right]dt = 0 \tag{13}$$

Where $(\cdot\cdot)$ represents the second derivative with respect to time and f_e is the density of reaction force of foundation. For the Pasternak foundation model

$$f_e = k_0 w - k_1\nabla^2 w \tag{14}$$

Where K_0 and K_s are the transverse and shear stiffness coefficients of the foundation, respectively. The stress resultants are given as

$$\begin{Bmatrix} N \\ M^{b} \\ M^{s} \end{Bmatrix} = \begin{bmatrix} A & B & B^{s} \\ A & D & D^{s} \\ B^{s} & D^{s} & H^{s} \end{bmatrix} \begin{Bmatrix} \varepsilon \\ k^{b} \\ k^{s} \end{Bmatrix}; \qquad S = A^{s}\gamma \tag{15}$$

Where

$$\begin{gathered} N = \{N_x, N_y, N_{xy}\}^t, \quad M^b = \{M^b_x, M^b_y, M^b_{xy}\}^t, \quad M^s = \{M^s_x, M^s_y, M^s_{xy}\}^t \\ \varepsilon = \{\varepsilon^0_x, \varepsilon^0_y, \varepsilon^0_{xy}\}^t, \quad k^b = \{k^b_x, k^b_y, k^b_{xy}\}^t, \quad k^s = \{k^s_x, k^s_y, k^s_{xy}\}^t \\ A = \begin{bmatrix} A_{11} & A_{12} & 0 \\ A_{12} & A_{22} & 0 \\ 0 & 0 & A_{66} \end{bmatrix}, \quad B = \begin{bmatrix} B_{11} & B_{12} & 0 \\ B_{12} & B_{22} & 0 \\ 0 & 0 & B_{66} \end{bmatrix}, \quad D = \begin{bmatrix} D_{11} & D_{12} & 0 \\ D_{12} & D_{22} & 0 \\ 0 & 0 & D_{66} \end{bmatrix} \\ B^s = \begin{bmatrix} B^s_{11} & B^s_{12} & 0 \\ B^s_{12} & B^s_{22} & 0 \\ 0 & 0 & B^s_{66} \end{bmatrix}, \quad D^s = \begin{bmatrix} D^s_{11} & D^s_{12} & 0 \\ D^s_{12} & D^s_{22} & 0 \\ 0 & 0 & D^s_{66} \end{bmatrix}, \quad H^s = \begin{bmatrix} H^s_{11} & H^s_{12} & 0 \\ H^s_{12} & H^s_{22} & 0 \\ 0 & 0 & H^s_{66} \end{bmatrix} \\ S = \{S^z_{xz}, S^s_{yz}\}^t, \quad \gamma = \{\gamma_{xz}, \gamma_{yz}\}^t, \quad A^s = \begin{bmatrix} A^s_{44} & 0 \\ 0 & A^s_{55} \end{bmatrix} \end{gathered} \tag{16}$$

And stiffness components and inertias are given as

$$\{A_{ij}, B_{ij}, C_{ij}, D_{ij}, E_{ij}, G_{ij}\} = \int_{-h/2-c}^{h/2-c} \{1, z_{ns}, f(z_{ns}), z^2_{ns}, z_{ns} f(z_{ns}), [f(z_{ns})]^2\} Q_{ij}\, dz_{ns} \tag{17}$$

$$(i, j = 1,2,6)$$

$$I_1, I_2, I_3, I_4, I_5, I_6 = \int_{-h/2-c}^{h/2-c} \rho(1, z_{ns}, z^2_{ns}, f(z_{ns}), z_{ns} f(z_{ns}), [f(z_{ns})]^2) dz_{ns} \tag{18}$$

For FG plates, the equilibrium equations take the forms

$$\begin{aligned} &A_{11}d_{11}u_0 + A_{66}D_{22}u_0 + (A_{12} + A_{66})d_{12}v_0 - B_{11}d_{11}w_b - (B_{12} + 2B_{66})d_{122}w_b \\ &- (B^s_{12} + 2B^s_{66})d_{122}w_s - B^s_{11}d_{111}w_s = I_0\ddot{u} \\ &A_{22}d_{22}v_0 + A_{66}d_{11}v_0 + (A_{12} + A_{66})d_{12}u_0 - B_{22}d_{222}w_b - (B_{12} + 2B_{66})d_{112}w_b \\ &- (B^s_{12} + 2B^s_{66})d_{112}w_s - B^s_{22}d_{222}w_s = I\ddot{v} \\ &B_{11}d_{111}u_0 + (B_{12} + 2B_{66})d_{122}u_0 + (B_{12} + 2B_{66})d_{112}v_0 + B_{22}d_{222}v_0 - D_{11}d_{1111}w_b \\ &- 2(D_{12} + 2D_{66})d_{1122}w_b - D_{22}d_{2222}w_b - D^s_{11}d_{1111}w_s - 2(D^s_{12} + 2D^s_{66})d_{1122}w_s \\ &- D^s_{22}d_{2222}w_s = I_0(\ddot{w}_b + \ddot{w}_s) - I_2\nabla^2\ddot{w}_b \\ &B^s_{11}d_{111}u_0 + (B^s_{12} + 2B^s_{66})d_{122}u_0 + (B^s_{12} + 2B^s_{66})d_{112}v_0 + B^s_{22}d_{222}v_0 - D^s_{11}d_{1111}w_b \\ &- 2(D^s_{12} + 2D^s_{66})d_{1122}w_b - D^s_{22}d_{2222}w_b - H^s_{11}d_{1111}w_s - 2(H^s_{12} + 2H^s_{66})d_{1122}w_s \\ &- H^s_{22}d_{2222}w_s + A^s_{55}d_{11}w_s + A^s_{44}d_{22}w_s = I_0(\ddot{w}_b + \ddot{w}_s) - \frac{I_2}{84}\nabla^2\ddot{w}_b \end{aligned} \tag{19}$$

where d_{ij}, d_{ijl}, and d_{ijlm} are the following differential operators

$$d_{ij} = \frac{\partial^2}{\partial x_i \partial x_j}, \qquad d_{ijl} = \frac{\partial^3}{\partial x_i \partial x_j \partial x_l}, \qquad d_{ijlm} = \frac{\partial^4}{\partial x_i \partial x_j \partial x_l \partial x_m}, \qquad (i, j, l, m = 1,2) \tag{20}$$

Following the Navier solution procedure, we assume the following solution form for u_0, v_0, w_b and w_s that satisfies the boundary conditions

$$\begin{Bmatrix} u_0 \\ v_0 \\ w_b \\ w_s \end{Bmatrix} = \sum_{m=1}^{\infty} \sum_{n=1}^{\infty} \begin{Bmatrix} U_{mn} \cos(\lambda x) \sin(\mu y) e^{i\omega t} \\ V_{mn} \sin(\lambda x) \cos(\mu y) e^{i\omega t} \\ W_{bmn} \sin(\lambda x) \sin(\mu y) e^{i\omega t} \\ W_{smn} \sin(\lambda x) \sin(\mu y) e^{i\omega t} \end{Bmatrix} \tag{21}$$

where $\lambda = m\pi / a$, $\mu = n\pi / b$ and U_{mn}, V_{mn}, W_{bmn}, W_{smn} being arbitrary parameters and ω denotes the eigenfrequency associated with (m,n)th eigenmode. One obtains the following operator equation

$$([K] - \omega^2 [M]\{\Delta\} = \{0\} \tag{22}$$

Where $\{\Delta\} = \{U, V, W_b, W_s\}^t$ and [K] and [M], stiffness and mass matrices, respectively, and represented as

$$[K] = \begin{bmatrix} a_{11} & a_{12} & a_{13} & a_{14} \\ a_{12} & a_{22} & a_{23} & a_{24} \\ a_{13} & a_{23} & a_{33} & a_{34} \\ a_{14} & a_{24} & a_{34} & a_{44} \end{bmatrix} \tag{23}$$

$$[M] = \begin{bmatrix} m_{11} & 0 & 0 & 0 \\ 0 & m_{22} & 0 & 0 \\ 0 & 0 & m_{33} & m_{34} \\ 0 & 0 & m_{34} & m_{44} \end{bmatrix} \tag{24}$$

In which

$$\begin{aligned} a_{11} &= A_{11}\alpha^2 + A_{66}\beta^2 \\ a_{12} &= \alpha\beta(A_{12} + A_{66}) \\ a_{13} &= -B_{11}a^3 \\ a_{14} &= C_{11}a^2 + C_{66}\beta^2 \\ a_{15} &= \alpha\beta(C_{12} + C_{66}) \\ a_{22} &= A_{66}\alpha^2 + A_{22}\beta^2 \\ a_{23} &= -B_{22}\beta^3 \\ a_{24} &= \alpha\beta(C_{12} + C_{66}) \\ a_{25} &= C_{66}\alpha^2 + C_{22}\beta^2 \end{aligned} \tag{25}$$

$$
\begin{aligned}
a_{33} &= D_{11}\alpha^4 + 2D_{12}\alpha^2\beta^2 + 4D_{66}\alpha^2\beta^2 + D_{22}\beta^4 + k_0 + k_1(\alpha^2+\beta^2)\\
a_{34} &= -E_{11}\alpha^3 - E_{12}\alpha\beta^2 - 2E_{66}\alpha\beta^2\\
a_{35} &= -E_{12}\alpha^2\beta - 2E_{66}\alpha^2\beta - E_{22}\beta^3\\
a_{44} &= F_{55} + G_{11}\alpha^2 + G_{66}\beta^2\\
a_{45} &= \alpha\beta(G_{12}+G_{66})\\
a_{55} &= F_{44} + G_{66}\alpha^2 + G_{22}\beta^2
\end{aligned}
\tag{25}
$$

And

$$\alpha = m\pi/a,\ \beta = n\pi/b \tag{26}$$

The natural frequencies of FG plate can be found from the nontrivial solution of Eq. (22).

5. Results

The refined shear deformation theory has been used to analyze the bending and free vibration of simply supported FG plates with porosities reposed on the elastic foundation for different values of gradient index, porosity volume fraction, foundations parameters, aspect and side-to-thickness ratios. The Navier solution procedure developed in the previous section is used to evaluate the Dimensionless deflections, stresses and natural frequencies. The following material properties are used in the analysis:

Material	Properties	
	E (N/m^2)	ρ (kg/m^3)
Aluminium (Al)	70×10^9	2707
Alumina (Al2O3)	380×10^9	3800
Zirconia (ZrO2)	151×10^9	3000
Ti-6Al-4V	105.7×10^9	4429
Aluminium oxide	320.2×10^9	3750

However, Poisson's ratio (ν) is assumed to be constant. The material properties of a perfect FG plate can be obtained when α is set to zero.

To validate accuracy of the proposed mathematical model for bending and vibration of the perfect FG plate (without porosity), the comparisons between the present results and the available results obtained by the exact 3-D of Vel *et al.* (2004), the refined shear deformation plate theory of Thai *et al.* (2011), Hosseini *et al.* (2011a) based on the Reddy's third-order shear deformation plate theory, A semi-analytical solution using the extended Kantorovich method together with infinite power series solution of Fallah *et al.* (2013), Dozio (2014) based on a family of two-dimensional shear and normal deformation theories with variable order, Neves *et al.* (2013) using a quasi-3D higher-order shear deformation theory and others available in literature. Excellent agreement is obtained for all cases.

Dimensionless deflections and stresses of simply supported Al/Al2O3 plates for different values of thickness ratio h/a, power law index k are listed in Tables 1 and 2. The calculated dimensionless deflections and stresses are compared with those reported by Neves *et al.* (2013),

Carrera *et al.* (2011), Thai *et al.* (2014), Zenkour *et al.* (2009) and Thai *et al.* (2014). Close agreements between the results are obtained for moderately thick plates and converge in the case of thick plates.

The results of nondimensional deflection of simply supported isotropic thin square plate under uniformly distributed load are presented in Table 3 for different values of foundation parameters K_0 and K_1. It can be seen that the present results converge with those given by Huang *et al.* (2008) and Thai *et al.* (2011).

Tables 4 and 5 present the comparisons of the fundamental frequency obtained from the present new plate theory with other plates theories results of Vel *et al.* (2004), Srinivas *et al.* (1970) and Thai *et al.* (2011) for different values of thickness-to-length ratio and foundation parameters K_0

Table 1 Dimensionless deflection and stress of square plates under sinusoidal loads (K_0=K_1=0)

P	Method	σ_x			$\overline{w}$		
		a/h=4	a/h=10	a/h=100	a/h=4	a/h=10	a/h=100
1	Neves (2013)	0.5911	1.4917	14.9450	0.7020	0.5868	0.5647
	Carrera (2011)	0.6221	1.5064	14.9690	0.7171	0.5875	0.5625
	Thai (2014)	0.5812	1.4898	14.9676	0.7284	0.5890	0.5625
	present	0.5803	1.4894	14.9675	0.7280	0.5889	0.5625
4	Neves (2013)	0.4330	1.1588	11.7370	1.1108	0.8700	0.8240
	Carrera (2011)	0.4877	1.1971	11.9230	1.1585	0.8821	0.8286
	Thai (2014)	0.4449	1.1794	11.9209	1.1599	0.8815	0.8287
	present	0.4423	1.1783	11.9208	1.1619	0.8818	0.8286
10	Neves (2013)	0.3097	0.8462	8.6010	1.3334	0.9888	0.9227
	Carrera (2011)	0.3695	0.8965	8.6077	1.3745	1.0072	0.9361
	Thai (2014)	0.3259	0.8785	8.9060	1.3909	1.0087	0.9362
	present	0.3234	0.8775	8.9058	1.3917	1.0089	0.9361

Table 2 Dimensionless deflections and stresses of rectangular plates under uniform loads (K_0=K_1=0)

P	Method	w^*	σ_x^*	σ_y^*	σ_{xy}^*
0	Zenkour (2009)	1.2583	0.7162	0.2448	0.2893
	Thai (2014)	1.2583	0.7160	0.2447	0.2890
	present	1.2582	0.7161	0.2494	0.2892
1	Zenkour (2009)	2.5133	0.3250	0.1111	0.1307
	Thai (2014)	2.5134	0.3250	0.1111	0.1306
	present	2.5133	0.3250	0.1125	0.1307
2	Zenkour (2009)	3.2267	0.4396	0.1502	0.1766
	Thai (2014)	3.2266	0.4395	0.1502	0.1766
	present	3.2267	0.4396	0.1522	0.1766
5	Zenkour (2009)	3.8517	0.5224	0.1785	0.2104
	Thai (2014)	3.8506	0.5223	0.1785	0.2103
	present	3.8517	0.5223	0.1818	0.2104

Table 3 Comparison of nondimensional deflection of simply supported isotropic thin square plate under uniformly distributed load

K_0	K_1	Huang (2008)	Thai (2011)	present
1	1	3.8546	3.855	4.0401
	3^4	0.763	0.763	0.7662
	5^4	0.1153	0.1153	0.1153
3^4	1	3.2105	3.2108	3.3327
	3^4	0.7317	0.7317	0.7344
	5^4	0.1145	0.1145	0.1145
5^4	1	1.4765	1.4765	1.4887
	3^4	0.5704	0.5704	0.5705
	5^4	0.1095	0.1095	0.1094

Table 4 Comparison study of fundamental frequency parameter for SSSS square plate (a/b=1) $\hat{\omega} = \omega a^2 \sqrt{\rho / E} / h$

h/a	Theory			% Diff
	Exact 3-D Vel (2004)	Exact 3-D Srinivas (1970)	Present	
h / a = 1 / 10	5.7769	5.7769	5.7695	0,1281
h / a = 1 / $\sqrt{10}$	4.6582	4.6582	4.6246	0,7213

Table 5 Dimensionless fundamental frequency $\hat{\omega} = \omega h \sqrt{\rho_{22} / E_{22}}$ of square plates. *P=0*

K_0	K_1	h/a	Method	
			Thai (2011)	Present
0	0	0.05	0.0291	0.0291
		0.1	0.1134	0.1133
		0.15	0.2452	0.2452
		0.2	0.4150	0.4150
0	100	0.05	0.0406	0.0405
		0.1	0.1597	0.1595
		0.15	0.3512	0.3499
		0.2	0.6075	0.6028
100	0	0.05	0.0298	0.0297
		0.1	0.1161	0.1161
		0.15	0.2516	0.2515
		0.2	0.4269	0.4266
100	100	0.05	0.0411	0.0410
		0.1	0.1617	0.1615
		0.15	0.3557	0.3544
		0.2	0.6156	0.6108

and K_1. As it can be seen, the new results are in good agreement with previous ones for moderately thick plates and converge in the case of thick plates. The shear (Pasternak) parameter has more effect on increasing the fundamental frequency than the Winkler parameter.

As another verification attempt, Tables 6 and 7 present respectively the comparisons of the lowest eight frequency parameters without elastic foundation (k_0=k_1=0) and fundamental natural frequency reposed on the Winkler foundation with Hosseini *et al.* (2011a), Lam *et al.* (2002) and Fallah *et al.* (2013). Close correlation is achieved for moderately thick plates and converge in the

Table 6 Lowest eight frequency parameters $\overline{\omega} = \omega a^2 \sqrt{\rho_0 h / G}$ rectangular plates

b/a	h/a	Method	Frequency parameters							
			(1,1)	(2,1)	(3,1)	(1,2)	(2,2)	(4,1)	(3,2)	(5,1)
0.5	0.01	Hosseini (2011a)	49.3032	78.8421	128.002	167.267	196.678	196.678	245.626	284.722
		present	49.3032	78.8422	128.0027	167.2673	196.6787	196.6787	245.6274	284.7232
	0.1	Hosseini (2011a)	45.4869	69.8093	106.735	133.720	152.753	152.753	182.565	204.956
		present	45.4917	69.8212	106.7652	133.7698	152.8208	152.8208	182.6670	205.0894
	0.2	Hosseini (2011a)	38.1883	55.2543	78.9865	95.2602	106.363	106.363	123.292	135.725
		present	38.2052	55.2943	79.0812	95.4108	106.5619	106.5619	123.5813	136.0940
	0.3	Hosseini (2011a)	31.6413	44.0236	60.6549	71.8663	79.4754	79.4754	83.4663	86.1806
		present	31.6739	44.0974	60.8216	72.1239	79.8093	79.8093	83.5322	86.1679
	0.4	Hosseini (2011a)	26.5910	36.1319	48.8370	57.4119	63.2548	63.2548	72.1987	77.6250
		present	26.6404	36.2404	49.0728	57.7687	63.7108	63.7108	72.8328	78.6020
1	0.01	Hosseini (2011a)	19.7320	49.3032	49.3032	78.8421	98.5169	98.5169	128.002	128.002
		present	19.7320	49.3032	49.3032	78.8422	98.5171	98.5171	128.0027	128.0027
	0.1	Hosseini (2011a)	19.0653	45.4869	45.4869	69.8093	85.0646	85.0646	106.735	106.735
		present	19.0660	45.4917	45.4917	69.8212	85.0829	85.0829	106.7652	106.7652
	0.2	Hosseini (2011a)	17.4523	38.1883	38.1883	55.2543	65.3135	65.3135	78.9865	78.9865
		present	17.4553	38.2052	38.2052	55.2943	65.3731	65.3731	79.0812	79.0812
	0.3	Hosseini (2011a)	15.5745	31.6413	31.6413	44.0236	51.1314	51.1314	60.6549	60.6549
		present	15.5806	31.6739	31.6739	44.0974	51.2391	51.2391	60.8216	60.8216
	0.4	Hosseini (2011a)	13.8136	26.5910	26.5910	36.1319	41.5668	41.5668	48.8370	48.8370
		present	13.8235	26.6404	26.6404	36.2404	41.7220	41.7220	49.0728	60.8216
2	0.01	Hosseini (2011a)	12.3342	19.7320	32.0572	41.9134	49.3032	49.3032	61.6149	71.4604
		present	12.3342	19.7320	32.0572	41.9134	49.3032	49.3032	61.6150	71.4604
	0.1	Hosseini (2011a)	12.0675	19.0653	30.3623	39.0977	45.4869	45.4869	55.8497	63.9008
		present	12.0677	19.0660	30.3643	39.1011	45.4917	45.4917	55.8571	63.9107
	0.2	Hosseini (2011a)	11.3717	17.4523	26.6838	33.4301	38.1883	38.1883	45.6412	51.2389
		present	11.3729	17.4553	26.6913	33.4424	38.2052	38.2052	45.6667	51.2723
	0.3	Hosseini (2011a)	10.4733	15.5744	22.924	28.0832	31.6413	31.6413	37.1114	41.1530
		present	10.4758	15.5806	22.9391	28.1071	31.6739	31.6739	37.1596	41.2153
	0.4	Hosseini (2011a)	9.54718	13.8136	19.7466	23.8151	26.5908	26.5908	30.8231	33.9311
		present	9.5513	13.8235	19.7703	23.8527	26.6404	26.6404	30.8953	34.0235

Table 7 Fundamental natural frequency of square isotropic plate $\bar{\omega} = \omega a^2 \sqrt{\rho_0 h / G}$; h/a=0.05

K_0	Lam (2002)	Fallah (2013)	present
0	19.74	19.56	19.5626
100	22.13	21.96	21.9600
1000	37.28	37.13	37.1232

Table 8 Comparison of fundamental frequency $\bar{\omega} = \omega h \sqrt{\rho_m / E_m}$ for square simply-supported Al/ZrO_2 plates. *a/h*=5

P	model							
	Vel (2004) Exact 3D	Dozio (2014) HOSNT-15	Dozio (2014) HOSNT-12	Dozio (2014) HOSNT-9	Neves (2013)	Qian (2004)	Hosseini (2011a)	present
2	0.2197	0.2196	0.2198	0.2225	0.2200	0.2153	0.2264	0.2187
3	0.2211	0.2211	0.2211	0.2245	0.2215	0.2172	0.2276	0.2183
5	0.2225	0.2225	0.2226	0.2263	0.2230	0.2194	0.2291	0.2174

Table 9 First 10 natural frequencies $\bar{\omega} = \omega h \sqrt{\rho_m / E_m}$ of square simply-supported Al/ZrO_2 plates with p=1 and various thickness ratios

a/h	model	mode									
		1	2	3	4	5	6	7	8	9	10
20	Dozio (2014) HOSNT-15	0.0154	0.0377	0.0377	0.0596	0.0740	0.0740	0.0950	0.0950	0.1030	0.1030
	Dozio (2014) HOSNT-12	0.0154	0.0377	0.0377	0.0596	0.0740	0.0740	0.0950	0.0950	0.1030	0.1030
	Dozio (2014) HOSNT-9	0.0154	0.0379	0.0379	0.0597	0.0742	0.0742	0.0955	0.0955	0.1030	0.1030
	Qian (2004)	0.0149	0.0377	0.0377	0.0593	0.0747	0.0747	0.0769	0.0912	0.0913	0.1029
	Neves (2013)	0.0153	0.0377	0.0377	0.0596	0.0739	0.0739	0.0950	0.0950	0.1030	0.1030
	present	0.0151	0.0373	0.0373	0.0591	0.0733	0.0733	0.0943	0.0943	0.1030	0.1030
10	Dozio (2014) HOSNT-15	0.0596	0.1425	0.1425	0.2059	0.2059	0.2191	0.2674	0.2674	0.2911	0.3359
	Dozio (2014) HOSNT-12	0.0596	0.1425	0.1425	0.2059	0.2059	0.2193	0.2674	0.2674	0.2911	0.3360
	Dozio (2014) HOSNT-9	0.0597	0.1435	0.1435	0.2059	0.2059	0.2213	0.2704	0.2704	0.2911	0.3405
	Qian (2004)	0.0584	0.1410	0.1410	0.2058	0.2058	0.2164	0.2646	0.2677	0.2913	0.3264
	Neves (2013)	0.0596	0.1426	0.1426	0.2059	0.2059	0.2193	0.2676	0.2676	0.2912	0.3364
	present	0.0591	0.1418	0.1418	0.2058	0.2058	0.2186	0.2671	0.2671	0.2911	0.3359
5	Dozio (2014) HOSNT-15	0.2191	0.4116	0.4116	0.4820	0.4820	0.5820	0.6996	0.8228	0.8281	0.8281
	Dozio (2014) HOSNT-12	0.2193	0.4116	0.4116	0.4824	0.4824	0.5820	0.7004	0.8228	0.8293	0.8293
	Dozio (2014) HOSNT-9	0.2213	0.4116	0.4116	0.4906	0.4906	0.5820	0.7159	0.8229	0.8496	0.8496
	Qian (2004)	0.2152	0.4114	0.4114	0.4761	0.4761	0.5820	0.6914	0.8192	0.8217	0.8242
	present	0.2186	0.4116	0.4116	0.4840	0.4840	0.5820	0.7046	0.8228	0.8349	0.8349

Table 10 Fundamental natural frequency $\bar{\omega} = \omega h\sqrt{\rho_{11}/E_{11}}$ of Al/Al_2O_3 FG plate (a/b=0.5)

h/a	K_0	K_1	P				
			0	1	2	5	10
0.1	0	0	0.0365	0.0246	0.0234	0.0213	0.0199
	0	100	0.1117	0.1168	0.1197	0.1211	0.1141
	100	0	0.0473	0.0408	0.0408	0.0405	0.0402
	100	100	0.1157	0.1212	0.1243	0.1211	0.1141
0.2	0	0	0.1376	0.0943	0.0888	0.0799	0.0747
	0	100	0.4356	0.3325	0.2879	0.2423	0.2283
	100	0	0.1813	0.1586	0.1582	0.1564	0.1556
	100	100	0.4356	0.3325	0.2879	0.2423	0.2283
0.3	0	0	0.2853	0.1987	0.1855	0.1644	0.1535
	0	100	0.6534	0.4988	0.4319	0.3634	0.3424
	100	0	0.3844	0.3420	0.3397	0.3339	0.3329
	100	100	0.6534	0.4988	0.4319	0.3634	0.3424

Table 11 Fundamental natural frequency $\bar{\omega} = \omega a^2\sqrt{\rho_0 h/G}$ of Al/Al_2O_3 FG plate (a/b=0.5, h/a=0.1)

P	K_0	K_1	Modes				
			(1,1)	(1,2)	(2,1)	(1,3)	(3,1)
0	0	0	0.0717	0.1133	0.2324	0.1805	0.4723
	0	100	0.2195	0.2851	0.4438	0.3777	0.7250
	100	0	0.0929	0.1277	0.2396	0.1898	0.4758
	100	100	0.2273	0.2911	0.4477	0.3823	0.7273
1	0	0	0.0485	0.0768	0.1589	0.1230	0.3274
	0	100	0.2295	0.2930	0.4381	0.3790	0.6766
	100	0	0.0802	0.0998	0.1710	0.1383	0.3332
	100	100	0.2382	0.2998	0.4427	0.3842	0.6794
5	0	0	0.0418	0.0660	0.1351	0.1050	0.2727
	0	100	0.2380	0.3011	0.4389	0.3838	0.6475
	100	0	0.0796	0.0944	0.1506	0.1246	0.2804
	100	100	0.2380	0.3011	0.4389	0.3838	0.6475
10	0	0	0.0392	0.0618	0.1264	0.0983	0.2547
	0	100	0.2242	0.2836	0.4135	0.3616	0.6100
	100	0	0.0791	0.0922	0.1433	0.1195	0.2632
	100	100	0.2242	0.2836	0.4135	0.3616	0.6100

case of thick plates. As it can be seen, with increases of aspect and thickness-to-length ratio, the natural frequency of vibration decreases and increases with increasing of the Winkler foundation.

In Tables 8 and 9, the comparison of the natural frequencies $\bar{\omega} = \omega h\sqrt{\rho_m / E_m}$ for square simply-supported Al/ZrO2 plates with those reported by Vel *et al.* (2004), Dozio (2014), Neves *et al.* (2013), Qian *et al.* (2004) and Hosseini *et al.* (2011a) are presented versus power law index and

thickness-to-length ratio. The results show that the effect of power law index on the natural frequency of vibration is very interesting.

From Tables 10 and 11 it is noticeable that the effect of the shear (Pasternak) parameter has more effect on increasing the natural frequency than the Winkler parameter. As it can be observed in the table, increasing the power law index increases the effect of the elastic foundation on the natural frequency. Increasing the power law index has a negligible effect on plate rested on Winkler elastic foundation.

Fig. 2 shows the effect of porosity on the Dimensionless center deflection versus side-to-thickness ratio a/h of an FGM plate. As it can be seen, the effect of porosity on the Dimensionless center deflection increases with the increase of the thickness ratio. Increasing value of porosity coefficient causes an increase in the Dimensionless center deflection.

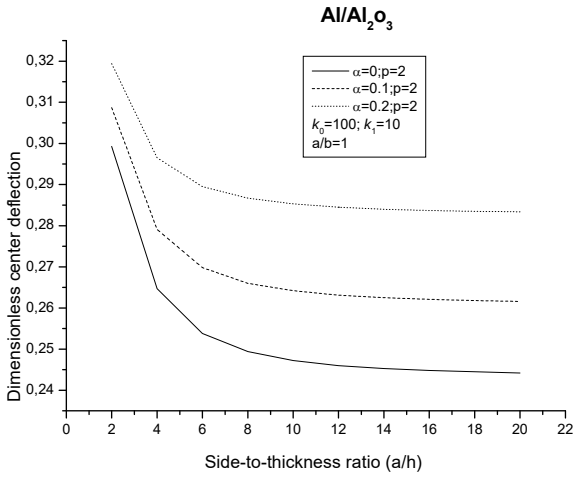

Fig. 2 Effect of the porosity on the Dimensionless center deflection through side-to-thickness ratio thickness of an FGM plate

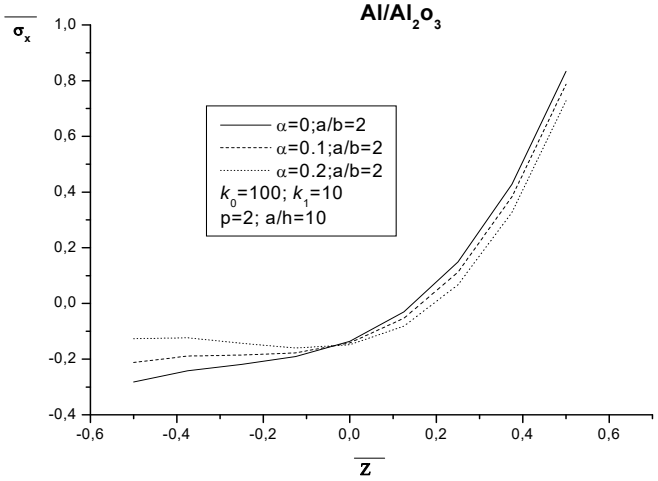

(a)

Fig. 3 Effect of the porosity on the In-plane longitudinal stress, the transversal shear stress and the longitudinal tangential stress through-the thickness of an FGM plate

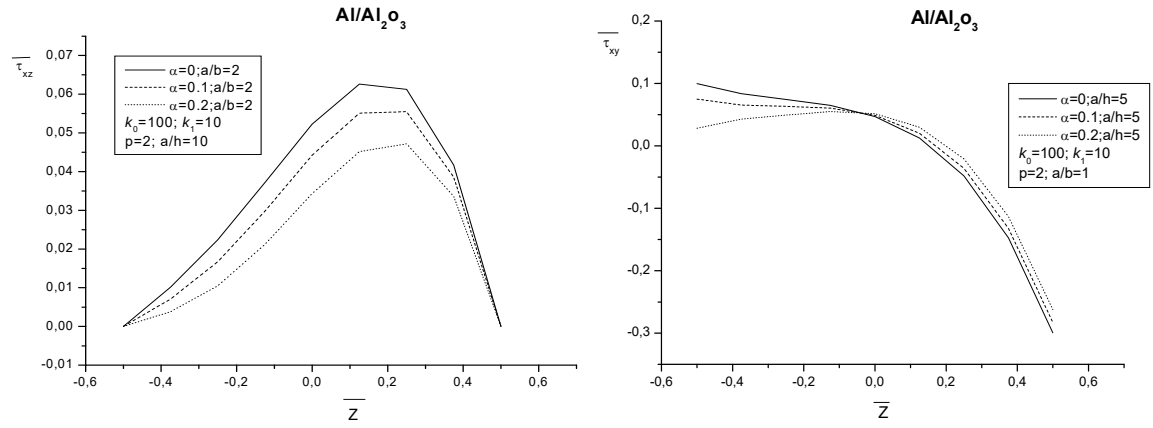

(b) (c)

Fig. 3 Continued

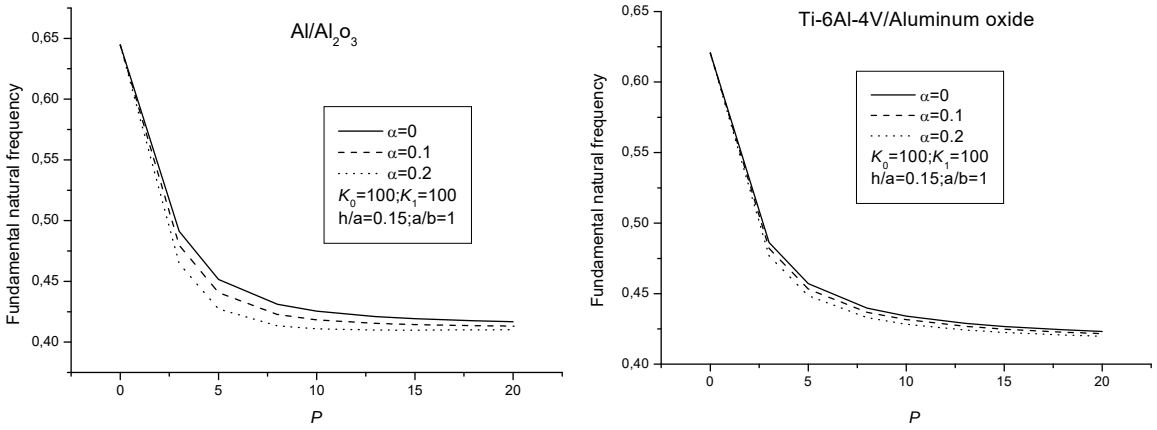

(a) (b)

Fig. 4 Effect of the porosity on the natural frequencies $\overline{\omega} = \omega h\sqrt{\rho_m / E_m}$ through the gradient index of an FGM plate

The effect of porosity on the in-plane longitudinal stress, the transversal shear stress and the longitudinal tangential stress through the thickness of an FGM plate is shown in Fig. 3. It can be seen that increasing value of porosity coefficient causes to decrease in the transversal shear stress. In Figs. 4(a) and (b), the fundamental natural frequency with three different types of porosity distribution are plotted according to the volume fraction index (P) for an Al/al_2O_3 and Ti-6Al-4V/Aluminum oxide FGM plate reposed on the elastic foundations. It is seen from these figures that, increasing values of porosity coefficient causes a decrease in the fundamental natural frequency.

Figs. 5(a) and (b), 6(a) and (b) represent variations of the fundamental natural frequency with several values of porosity coefficient versus the thickness-to-length ratio (h/a) and aspect ratio respectively. The FGM plates are reposed on the Winkler-Pasternak foundation. The figures show that increasing in the thickness-to-length ratio increases the effect of the porosity on the natural

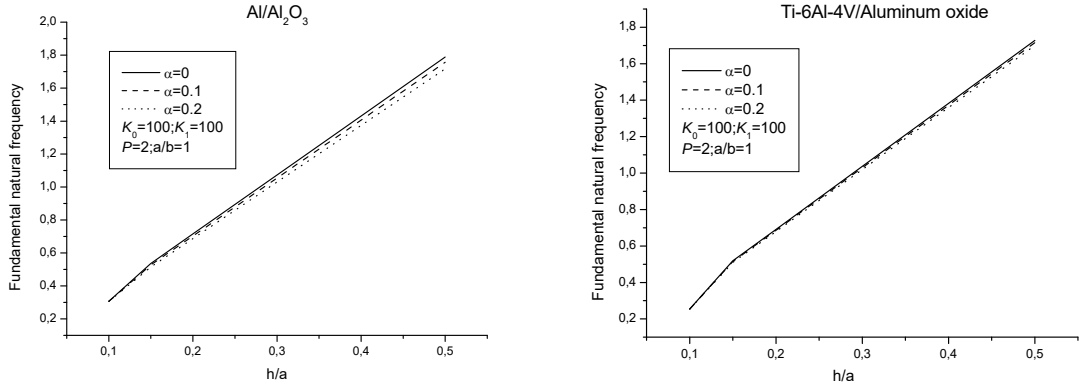

(a) (b)

Fig. 5 Effect of the porosity on the natural frequencies $\bar{\omega} = \omega h\sqrt{\rho_m / E_m}$ through the side-to-thickness ratio of an FGM plate

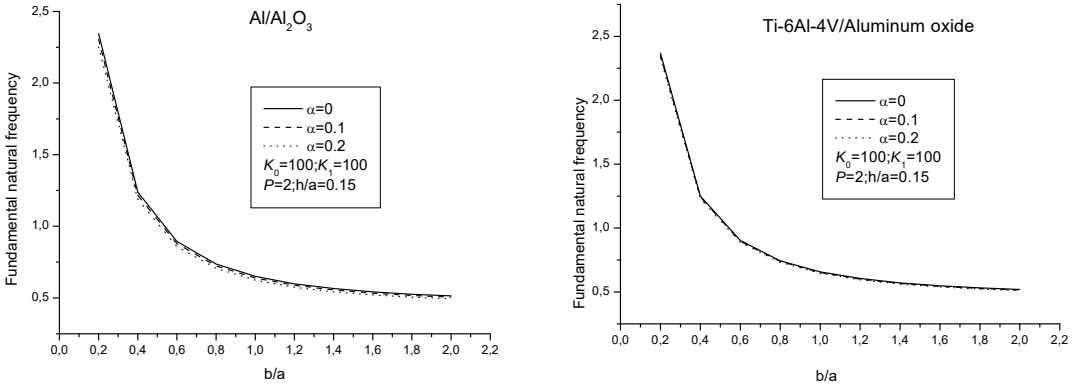

(a) (b)

Fig. 6 Effect of the porosity on the fundamental natural frequencies $\bar{\omega} = \omega a^2\sqrt{\rho_0 h / G}$ through the aspect ratio of an FGM plate

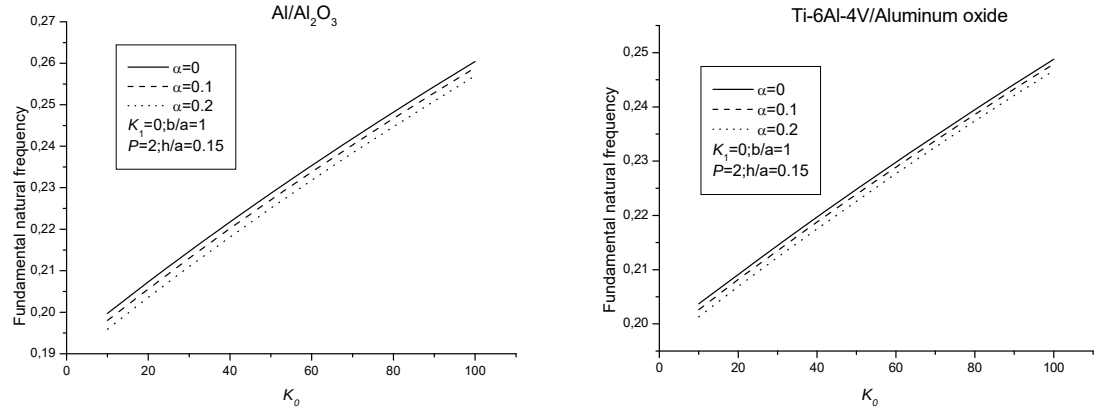

(a) (b)

Fig. 7 Effect of the porosity on the fundamental natural frequencies $\bar{\omega} = \omega a^2\sqrt{\rho_0 h / G}$ reposed on the Winkler foundation of an FGM plate

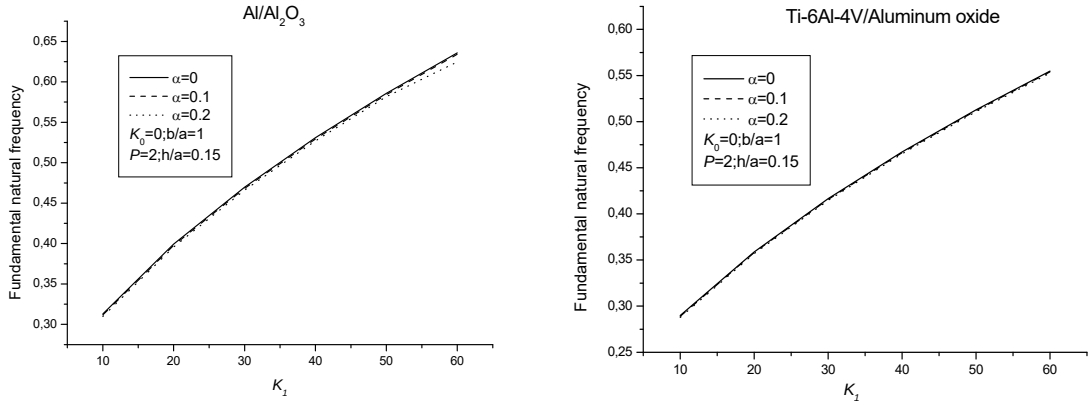

Fig. 8 Effect of the porosity on the fundamental natural frequencies $\bar{\omega} = \omega a^2 \sqrt{\rho_0 h / G}$ reposed on the Pasternak foundation of an FGM plate

frequency. Increasing in the aspect ratio leads to a decrease in the natural frequency.

The effect of the Winkler K_0 and Pasternak K_1 parameters with three different types of porosity coefficient on the fundamental natural frequency of two FGM plate types (Al_2O_3, Ti-6Al-4V/Aluminum oxide) are shown in Figs. 7(a) and (b), 8(a) and (b). As it can be seen, the shear (Pasternak) parameter has more effect on increasing the fundamental frequency than the Winkler parameter. The effect of the porosity coefficient of the plate reposed on the Winkler foundation is higher than the plate reposed on the Pasternak foundation.

6. Conclusions

An extensive study of the bending and free vibration analysis of functionally graded perfect and imperfect plates resting on two-parameter elastic foundation with shear effect is presented. It is based on the neutral surface position and the use of a new refined shear deformation theory. The material properties are assumed to vary according to the thickness direction of the plate and the rule of mixture which was reformulated to assess the material characteristics with the porosity phases. The Navier method is used for the analytical solutions of the functionally graded plate with simply supported boundary conditions. Convergence and validation studies have been carried out to prove the accuracy of the present theory. The obtained results show a good agreement with those available in the literature for moderately thick plates. The following conclusions were noticed from the typical results obtained for different volume fraction indices, the aspect ratios, the thickness ratios, the foundation stiffness parameters and three values of the porosity coefficient.

• The shear (Pasternak) parameter has more effect on increasing the fundamental frequency than the Winkler parameter.

• The natural frequency of vibration decreases with increase of the aspect and the thickness-to-length ratios.

• The effect of power law index on the natural frequency of vibration is very interesting.

• Increasing the power law index increases the effect of the elastic foundation on the natural frequency.

• Increasing the power law index has a negligible effect on plate rested on Winkler elastic foundation.

• Increasing the value of porosity coefficient causes an increase in Dimensionless center deflection and a decrease in the transversal shear stress and the fundamental natural frequency.

• Increasing in the thickness-to-length ratio increases the effect of the porosity on the Dimensionless center deflection and natural frequency.

• The effect of the porosity coefficient of the plate reposed on the Winkler foundation is higher than plate reposed on the Pasternak foundation.

References

Ait Atmane, H., Tounsi, A. and Bernard, F. (2015a), "Effect of thickness stretching and porosity on mechanical response of a functionally graded beams resting on elastic foundations", *Int. J. Mech. Mater*., 1-14.

Ait Atmane, H., Tounsi, A., Bernard, F. and Mahmoud, S.R. (2015b), "A computational shear displacement model for vibrational analysis of functionally graded beams with porosities", *Steel Compos. Struct*., **19**(2), 369-385.

Ait Yahia, S., Ait Atmane, H., Houari, M.S.A. and Tounsi, A. (2015), "Wave propagation in functionally graded plates with porosities using various higher-order shear deformation plate theories", *Struct. Eng. Mech*., **53**(6), 1143-1165.

Bakora, A. and Tounsi, A. (2015), "Thermo-mechanical post-buckling behavior of thick functionally graded plates resting on elastic foundations", *Struct. Eng. Mech*., **56**(1), 85-106.

Belabed, Z., Houari, M.S.A., Tounsi, A., Mahmoud, S.R. and Anwar, B.O. (2014), "An efficient and simple higher order shear and normal deformation theory for functionally graded material (FGM) plates", *Composites: Part B.*, **60**, 274-283.

Bennai, R., Ait Atmane, H. and Tounsi, A. (2015), "A new higher-order shear and normal deformation theory for functionally graded sandwich beams", *Steel Compos. Struct.*, **19**(3), 521-546.

Brischetto, S. and Carrera, E. (2010), "Advanced mixed theories for bending analysis of functionally graded plates", *Comput. Struct.*, **88**(23-24), 1474-1483.

Brischetto, S. (2013), "Exact elasticity solution for natural frequencies of functionally graded simply-supported structures", *Comput. Model. Eng. Sci.*, **95**(5), 391-430.

Bodaghi, M. and Saidi, A.R. (2011), "Stability analysis of functionally graded rectangular plates under nonlinearly varying in-plane loading resting on elastic foundation", *Arch. Appl. Mech*., **81**(6), 765-780.

Bousahla, A.A., Houari, M.S.A., Tounsi, A. and Adda Bedia, E.A. (2014), "A novel higher order shear and normal deformation theory based on neutral surface position for bending analysis of advanced composite plates", *Int. J. Comput. Meth.*, **11**(6), 1350082.

Carrera, E., Brischetto, S., Cinefra, M. and Soave, M. (2010), "Refined and advanced models for multilayered plates and shells embedding functionally graded material layers", *Mech. Adv. Mater. Struct.*, **17**(8), 603-621.

Carrera, E., Brischetto, S., Cinefra, M. and Soave, M. (2011), "Effects of thickness stretching in functionally graded plates and shells", *Compos Part B: Eng.*, **42**(2), 123-133.

Dozio, L. (2014), "Exact free vibration analysis of Lévy FGM plates with higher-order shear and normal deformation theories", *Compos. Struct*., **111**(1), 415-425.

Efraim, E. and Eisenberger, M. (2007), "Exact vibration analysis of variable thickness thick annular isotropic and FGM plates", *J. Sound Vib.*, **299**(4), 720-738.

Fallah, A., Aghdam, M.M. and Kargarnovin, M.H. (2013), "Free vibration analysis of moderately thick functionally graded plates on elastic foundation using the extended Kantorovich method", *Arch. Appl. Mech*., **83**(2), 177-191.

Fazzolari, F.A. and Carrera, E. (2014), "Coupled thermoelastic effect in free vibration analysis of anisotropic multilayered plates and FGM plates by using a variable-kinematics Ritz formulation", *Eur. J. Mech. A/Solid.*, **44**, 157-174.

Hadji, L. and Adda Bedia, E.A. (2015a), "Influence of the porosities on the free vibration of FGM beams", *Wind Struct.*, **21**(3), 273-287.

Hadji, L., Hassaine Daouadji, T. and Adda Bedia, E.A. (2015b), "A refined exponential shear deformation theory for free vibration of FGM beam with porosities", *Geomech. Eng*., **9**(3), 361-372

Hamidi, A., Houari, M.S.A., Mahmoud, S.R. and Tounsi, A. (2015), "A sinusoidal plate theory with 5-unknowns and stretching effect forthermomechanical bending of functionally graded sandwich plates", *Steel Compos. Struct.*, **18**(1), 235-253.

Hasani Baferani, A., Saidi, A.R. and Ehteshami, H. (2011), "Accurate solution for free vibration analysis of functionally graded thick rectangular plates resting on elastic foundation", *Compos. Struct*., **93**(7), 1842-1853.

Hirai, T. (1996), "Functional gradient materials", *Proc. Ceramics-Part 2 in Mater. Sci. Technol.*, **17B**, 293-341.

Huang, Z.Y., Lu, C.F. and Chen, W.Q. (2008), "Benchmark solutions for functionally graded thick plates resting on Winkler-Pasternak elastic foundations", *Compos. Struct*., **85**(2), 95-104.

Hosseini-Hashemi, S., Fadaee, M. and Atashipour, S.R. (2011a), "A new exact analytical approach for free vibration of Reissner-Mindlin functionally graded rectangular plates", *Int. J. Mech. Sci*., **53**(1), 11-22.

Hosseini-Hashemi, S., Fadaee, M. and Taher, H.R.D. (2011b), "Exact solutions for free flexural vibration of Lévy-type rectangular thick plates via third-order shear deformation plate theory", *Appl. Math. Model.*, **35**(2), 708-727.

Gan, B.S., Trinh, T.H., Le, T.H. and Nguyen, D.K. (2015), "Dynamic response of non-uniform Timoshenko beams made of axially FGM subjected to multiple moving point loads", *Struct. Eng. Mech*., **53**(5), 981-995.

Kitipornchai, S., Yang, J. and Liew, K.M. (2004), "Semi-analytical solution for nonlinear vibration of laminated FGM plates with geometric imperfections", *Int. J. Solid. Struct*., **41**(9-10), 2235-2257.

Lam, K.Y., Wang, C.M. and He, X.Q. (2002), "Canonical exact solutions for Levy-plates on two parameter foundation using Green's functions", *Eng. Struct.*, **22**(4), 364-378.

Meksi, A., Benyoucef, S., Houari, M.S.A and Tounsi, A. (2015), "A simple shear deformation theory based on neutral surface position for functionally graded plates resting on Pasternak elastic foundations", *Struct. Eng. Mech*., **53**(6)**,** 1215-1240.

Neves, A.M.A., Ferreira, A.J.M., Carrera, E., Cinefra, M., Roque, C.M.C., Jorge, R.M.N. and Soares, C.M.M. (2013), "Static, free vibration and buckling analysis of isotropic and sandwich functionally graded plates using a quasi-3D higher-order shear deformation theory and a meshless technique", *Compos. Part B: Eng.*, **44**(1), 657-674.

Nguyen, D.D. and Pham, H.C. (2013), "Nonlinear postbuckling of symmetric S-FGM plates resting on elastic foundations using higher order shear deformation plate theory in thermal environments", *Compos. Struct.*, **100**, 566-574.

Pasternak, P.L. (1954), "On a new method of analysis of an elastic foundation by means of two foundation constants", *Gosudarstvennoe Izdatelstvo Literaturi po Stroitelstvu I Arkhitekture Moscow USSR*, 1-56. (in Russian)

Pindera, M.J., Arnold, S.M., Aboudi, J. and Hui, D. (1994), "Use of composite in functionnaly graded materials", *Compos. Eng.*, **4**(1), 1-145.

Pradhan, K.K. and Chakraverty, S. (2015), "Free vibration of functionally graded thin elliptic plates with various edge support", *Struct. Eng. Mech*., **53**(2), 337-354.

Prakash, T., Singha, M.K. and Ganapathi, M. (2009), "Influence of neutral surface position on the nonlinear stability behavior of functionally graded plates", *Comput. Mech.*, **43**(3), 341-350.

Qian, L.F., Batra, R.C. and Chen, L.M. (2004), "Static and dynamic deformations of thick functionally graded elastic plates by using higher-order shear and normal deformable plate theory and meshless local Petrov-Galerkin method", *Composites: Part B*., **35**(6), 685-697.

Srinivas, S., Joga Rao, C.V. and Rao, A.K. (1970), "An exact analysis for vibration of simply-supported homogeneous and laminated thick rectangular plates", *J. Sound. Vib.*, **12**(2), 187-199.
Talha, M. and Singh, B.N. (2010), "Static response and free vibration analysis of FGM plates using higher order shear deformation theory", *Appl. Math. Model.*, **34**(12), 3991-4011.
Thai, H.T. and Choi, D.H. (2011), "A refined plate theory for functionally graded plates resting on elastic foundation", *Compos. Sci. Technol*., **71**(16), 1850-1858.
Thai, H.T. and Choi, D.H. (2012), "A refined shear deformation theory for free vibration of functionally graded plates on elastic foundation", *Composites: Part B.*, **43**(5), 2335-2347.
Thai, H.T. and Choi, D.H. (2014), "Zeroth-order shear deformation theory for functionally graded plates resting on elastic foundation", *Int. J. Mech. Sci*., **78**, 35-43.
Tounsi, A., Houari, M.S.A., Benyoucef, S. and Adda Bedia, E.A. (2013), "A refined trigonometric shear deformation theory for thermoelastic bending of functionally graded sandwich plates", *Aero. Sci. Technol.*, **24**(1), 209-220.
Vel, S.S. and Batra, R.C. (2004), "Three-dimensional exact solution for the vibration of functionally graded rectangular plates", *J. Sound Vib.*, **272**(3), 703-730.
Wattanasakulpong, N., Gangadhara Prusty, B., Kelly, D.W. and Hoffman, M. (2012), "Free vibration analysis of layered functionally graded beams with experimental validation", *Mater. Des.*, **36**, 182-190.
Wattanasakulponga, N. and Ungbhakornb, V. (2014), "Linear and non linear vibration analysis of elastically restrained ends FGM beams with porosities", *Aero. Sci. Technol*., **32**(1), 111-120.
Zenkour, A.M., Mashat, D.S. and Elsiba, K.A. (2009), "Bending analysis of functionally graded plates in the context of different theories of thermoelasticity", *Math. Prob. Eng.*, 962351.
Zhang, D.G. and Zhou, Y.H. (2008), "A theoretical analysis of FGM thin plates based on physical neutral surface", *Comput. Mater. Sci.*, **44**(2), 716-720.
Zhu, J., Lai, Z., Yin, Z., Jeon, J. and Lee, S. (2001), "Fabrication of ZrO2-NiCr functionally graded material by powder metallurgy", *Mater. Chem. Phys.*, **68**(1-3)**,** 130-135.

CC